1

2

3

Unbiased interrogation of memory B cells from convalescent COVID-19 patients

reveals a broad antiviral humoral response targeting SARS-CoV-2 antigens

beyond the spike protein

7

Jillian M. DiMuzio[1][*], Baron C. Heimbach[1], Raymond J. Howanski[1], John P. Dowling[1], Nirja

B. Patel[1], Noeleya Henriquez[1], Chris Nicolescu[1], Mitchell Nath[1], Antonio Polley[1], Jamie

L. Bingaman[1], Todd Smith[1], Benjamin C. Harman[1], Matthew K. Robinson[1], Michael J.

Morin[1] and Pavel A. Nikitin[1]

12

[1]Immunome, Inc., Exton, PA, U.S.A.

14

*Corresponding author

Email: jdimuzio@immunome.com

17

18

19

20

21

22

23

24

Abstract

26

Patients who recover from SARS-CoV-2 infections produce antibodies and antigen-specific T cells against multiple viral proteins. Here, an unbiased interrogation of the anti-viral memory B cell repertoire of convalescent patients has been performed by generating large, stable hybridoma libraries and screening thousands of monoclonal antibodies to identify specific, high-affinity immunoglobulins (Igs) directed at distinct viral components. As expected, a significant number of antibodies were directed at the Spike (S) protein, a majority of which recognized the full-length protein. These full-length Spike specific antibodies included a group of somatically hypermutated IgMs. Further, all but one of the six COVID-19 convalescent patients produced class-switched antibodies to a soluble form of the receptor-binding domain (RBD) of S protein. Functional properties of anti-Spike antibodies were confirmed in a pseudovirus neutralization assay. Importantly, more than half of all of the antibodies generated were directed at non-S viral proteins, including structural nucleocapsid (N) and membrane (M) proteins, as well as auxiliary open reading frame-encoded (ORF) proteins. The antibodies were generally characterized as having variable levels of somatic hypermutations (SHM) in all Ig classes and sub-types, and a diversity of V_L and V_H gene usage. These findings demonstrated that an unbiased, function-based approach towards interrogating the COVID-19 patient memory B cell response may have distinct advantages relative to genomics-based approaches when identifying highly effective anti-viral antibodies directed at SARS-CoV-2.

46

47

INTRODUCTION

49

As the one-year mark approaches since its emergence in Wuhan, China in late 2019 [1], the prolonged spread of the severe acute respiratory syndrome coronavirus 2 (SARS-CoV-2) virus has resulted in one of the most devastating global health challenges of the last century [2–4]. With greater than 45 million confirmed cases and nearly 1.2 million deaths world-wide (WHO, as of November 2020 [5]), the virus continues to pose an extraordinary challenge to the scientific community, consequently becoming an unprecedented socio-economic disaster and burdening healthcare systems around the world. Infection with SARS-CoV-2 results in a myriad pathologies [6] collectively referred to as COVID-19 [3]. While a majority of individuals who become infected with the virus are capable of generating a productive anti-viral response, for many their anti-viral humoral response will not be sufficient to shield them from a potentially deadly infection. Therefore, as the global community braces for the next spike in infection and mortality rates, the urgency to develop effective therapeutics recapitulating the productive anti-viral response to combat the swelling health crisis has never been greater.

64

SARS-CoV-2 genomic RNA contains a large viral replicase gene, genes encoding non-structural proteins at its 5' end, and a region encoding four major structural and multiple accessory proteins at the 3' end. Structural proteins include Spike or Surface glycoprotein (S), Membrane protein (M), Envelope protein (E) and Nucleocapsid protein (N) [7]. The membrane surface glycoprotein S consists of two subunits, S1 and S2, that mediate viral

70   binding to the host receptor ACE2 and fusion with the host cell membrane, respectively.

71   The S1 subunit contains the receptor binding domain (RBD) that directly interacts with

72   ACE2 and is a target of multiple neutralizing antibodies currently in clinical trials [8,9].

73   Genetic analyses of immune effector cells from convalescent patients who had effectively

74   cleared the SARS-CoV-2 virus revealed that these individuals often had robust T and B

75   cell responses to multiple other viral antigens beyond S protein [10–14], suggesting that

76   the recognition of multiple antigens beyond the S protein may be important for viral

77   clearance and the efficient resolution of infection. Included among the targets of the

78   adaptive immune response were N and M proteins, as well as proteins encoded by the

79   viral open reading frame (ORF). As such, a multi-targeted mixture of high-affinity anti-

80   SARS-CoV-2-specific antibodies, more reflective of the broad humoral response seen in

81   high-titer, mild to moderate COVID-19 convalescent patients, may be a more effective

82   therapeutic strategy than using S-specific antibodies alone.

83   This report describes studies to elucidate the memory B cell antibody response in

84   convalescent patients, using a method that enables the generation of large, stable

85   hybridoma libraries from primary human B cells. This approach was previously used to

86   identify a panel of monoclonal antibodies from convalescent patients infected with natural

87   polio virus (PV), oral PV-vaccinated and inactivated PV-boosted healthy subjects [15–

88   17], and, most recently, an anti-amyloid antibody with the anti-biofilm activity [18] from a

89   hybridoma library generated with memory B cells from an Alzheimer's Disease patient

90   [19]. In the current report, eleven hybridoma libraries were generated from the memory B

91   cells of six COVID-19 patients. These libraries were comprised of more than 150 distinct

92   monoclonal antibodies that were selected on the basis of their binding to multiple SARS-

93   CoV-2 proteins in both cell-based and target-based screens. Characterization of these

94   antibodies revealed broad responses to diverse viral antigens. Fewer than half of the

95   antibodies were directed at S protein, while the remainder were directed at other viral

96   proteins including N and ORF-encoded proteins. Even though the antibodies were

97   directed at highly diverse SARS-CoV-2 antigens, they were generally characterized as

98   having variable levels of somatic hypermutation (SHM) and a diversity of V_L and V_H gene

99   usage. Functional properties of anti-Spike antibodies were successfully confirmed in a

100   pseudovirus neutralization assay. These results indicate that an unbiased interrogation

101   of COVID-19 patient B cell repertoires is an effective approach to identifying specific anti-

102   viral antibodies and antibody mixtures with the desired binding and functional properties.

103   Antibodies identified and characterized in this manner could be recombinantly produced

104   to yield therapeutic or prophylactic products to address the COVID-19 pandemic. The

105   rapidity with which antibodies from convalescent patients can be identified and

106   characterized suggests that this platform could be a useful component of a rapid response

107   to future pandemics.

108

109   **RESULTS**

110

111   **Evaluating the breadth of patients' humoral responses against SARS-CoV-2**

112

113   We examined the overall spectrum of the productive antibody response to SARS-CoV-2

114   using an automated, high-throughput hybridoma library generation and screening

115 platform [15] after isolating memory B cells acquired from blood samples of COVID-19

116 convalescent patients who demonstrated a high (2880) antibody titer to N and/or S

117 proteins. More than 17,000 hybridomas were generated from the memory B cells of six

118 patients (Table 1), and the naturally occurring human antibodies (IgM, IgG, and IgA

119 isotypes) secreted by those hybridomas were screened for reactivity against a panel of

120 SARS-CoV-2 proteins. Antibody screening assays were developed for three structural

121 proteins (S, N, M) and a panel of accessory ORF proteins of SARS-CoV-2 (Table 2). The

122 screening assays included a rapid and sensitive homogeneous time resolved

123 fluorescence (hTRF) assay that used soluble recombinant viral proteins (Figure 1), as

124 well as a selective, cell-based flow cytometry assay that allowed probing of antibodies to

125 transiently transfected viral antigens expressed within the context of human cells (Figure

126 2). Commercially available antibodies specific for SARS-CoV-2 proteins demonstrated

127 selective and saturable binding in both assays. The dynamic ranges varied among the

128 specific targets and between assays (Figure 1 and Figure 2) within a 10 pM-100 nM

129 window. Viral protein expression in the cell-based assay was additionally confirmed by

130 Western blot. For cell-based assays, using commercially available controls, the

131 localization of the C-terminus truncated Spike protein (S delta 19aa) was confirmed to be

132 on the surface of the transfected cells, while the localization for Nucleocapsid,

133 Membrane, ORF3a, ORF6, ORF7a, ORF8, and ORF10 proteins was predominantly

134 intracellular.

135

Patient ID	Gender	Age
T_00292	Male	31
T_00293	Female	44
T_00294	Female	34
T_00295	Female	53
T_00298	Female	46
T_00302	Male	45

Table 1: Convalescent plasma donors

SARS-CoV-2 Viral Targets		Assay System	
Spike (S)		HTRF	Cell-based
1	Trimer-stabilized FL (non-S1)	√	
2	S1 domain (non-RBD)	√	
3	Receptor binding domain (RBD)	√	√
4	S delta 19aa		√
Nucleocapsid (N)		√	√
Envelope (E)		√	√
Membrane (M)		√	√
ORF3a		√	√
ORF6			√
ORF7a			√
ORF8		√	√
ORF10			√

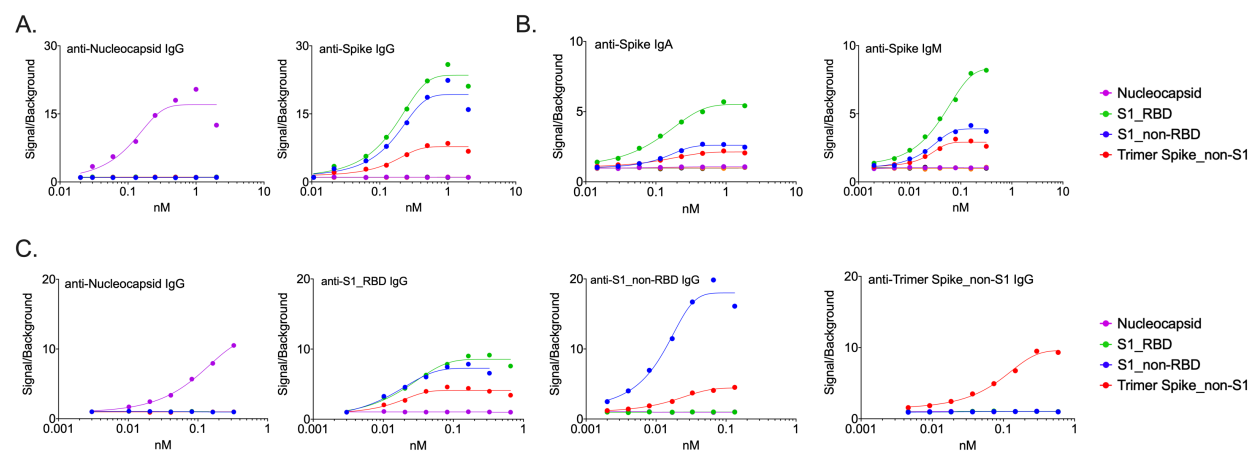Table 2: SARS-CoV-2 viral target panel for screening

7

Figure 1. Homogeneous Time Resolved Fluorescence Assay (hTRF) for detection of anti-viral antibodies. (A) Dynamic range and antigen specificity exhibited by Spike and Nucleocapsid control antibodies. (B) Detection of various Spike protein domains with control antibodies of varying isotypes in the hTRF assay. (C) Patient-derived antibodies exhibit specificity and high affinity for target proteins in the hTRF assay.
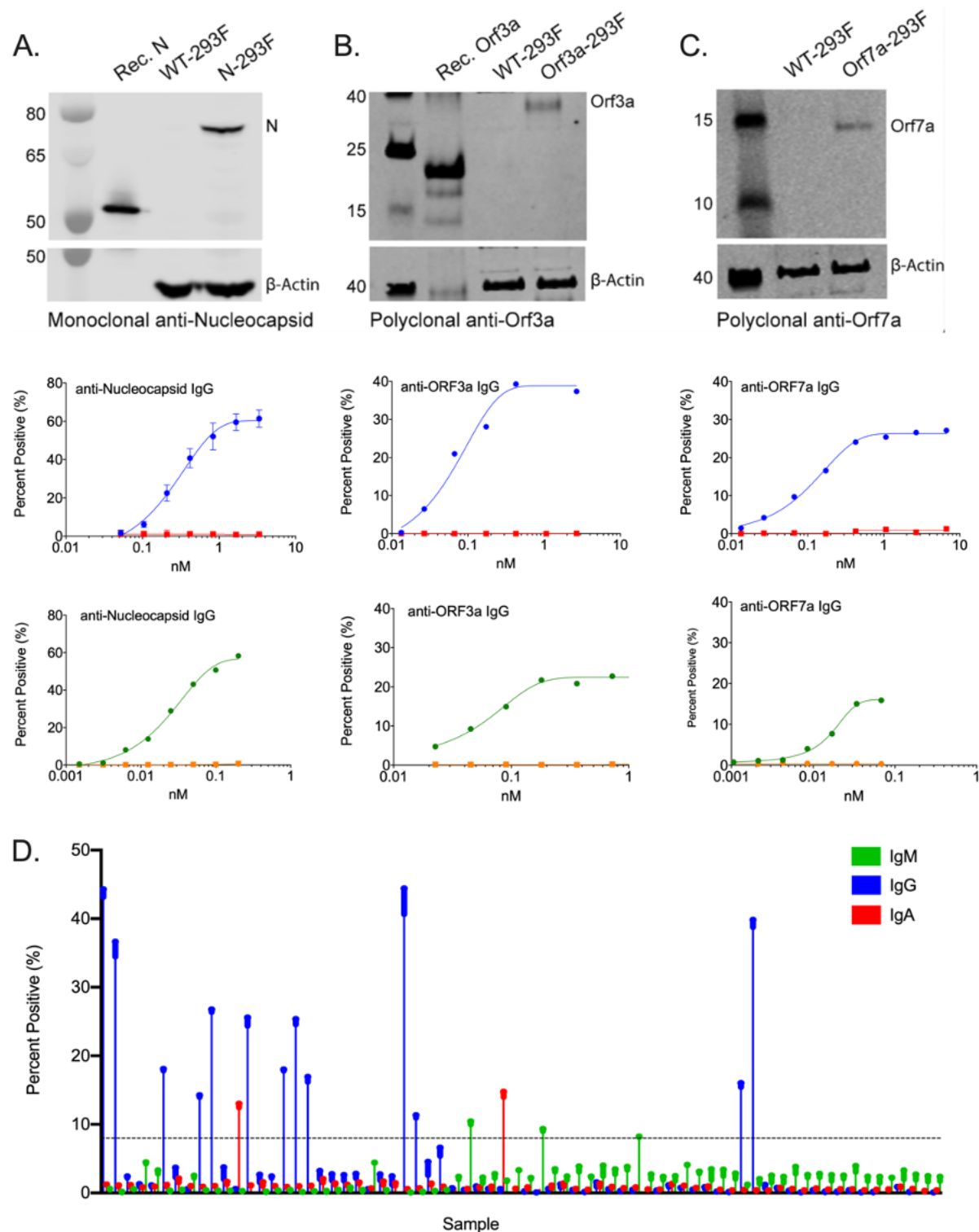
149

Figure 2. Detection of viral proteins in a cell-based expression system. Commercially available control antibodies were used to detect SARS-CoV-2 protein expression in

152   transiently transfected cells by Western blot (top row) and in a concentration-dependent

153   manner by flow cytometry (middle row). Where available, recombinant protein was used

154   as a positive control for Western blots. Mock-transfected cells served as a negative

155   control for flow-cytometry studies. Patient-derived antibodies demonstrate specificity to

156   antigen-specific cell lines relative to mock-transfected cells (bottom row). (A)

157   Nucleocapsid protein. (B) ORF3a protein. (C) ORF7a protein. (D) Primary screening data

158   depicting isotype-specific detection of patient-derived anti-spike antibodies by flow

159   cytometry.

160

161   **Convalescent patients develop antibodies against a broad array of viral proteins**

162

163   Consistent with previous reports [12,14], S protein was identified as the major antigen for

164   antibody responses in these patients. As shown in Figure 3A, S represented the single

165   most frequently identified target: 76 (44%) of the mono-specific antibodies bound

166   selectively to S protein. As expected, the epitopes for anti-Spike antibodies were

167   distributed across the RBD, non-RBD S1, and non-S1 regions of the Spike protein (Figure

168   3B). However, consistent with the hypothesis that patients would be mounting antibody

169   responses to a broad range of SARS-CoV-2 proteins, more than half (56%) of identified

170   antibodies bound to non-Spike viral antigens (Figure 3). ORF8 - (28 antibodies, 17%) and

171   N - (23 antibodies, 14%) specific antibodies represented the second and third most-

172   frequently identified targets, respectively. Of note, the antibodies identified in the hTRF

173   assay were biased toward the IgG class (>80%) (Figure 4A). This bias was likely due to

174   lack of sensitivity in the assay for either IgA or IgM, as demonstrated in the control

175   antibody titrations shown in Figure 1. While IgG was still the predominant isotype (~50%)

176   in the cell-based screening, IgA (~20%) and IgM (~30%) antibodies were also well-

177   represented (Figure 4B). Further, these isotypes were also spread across the landscape

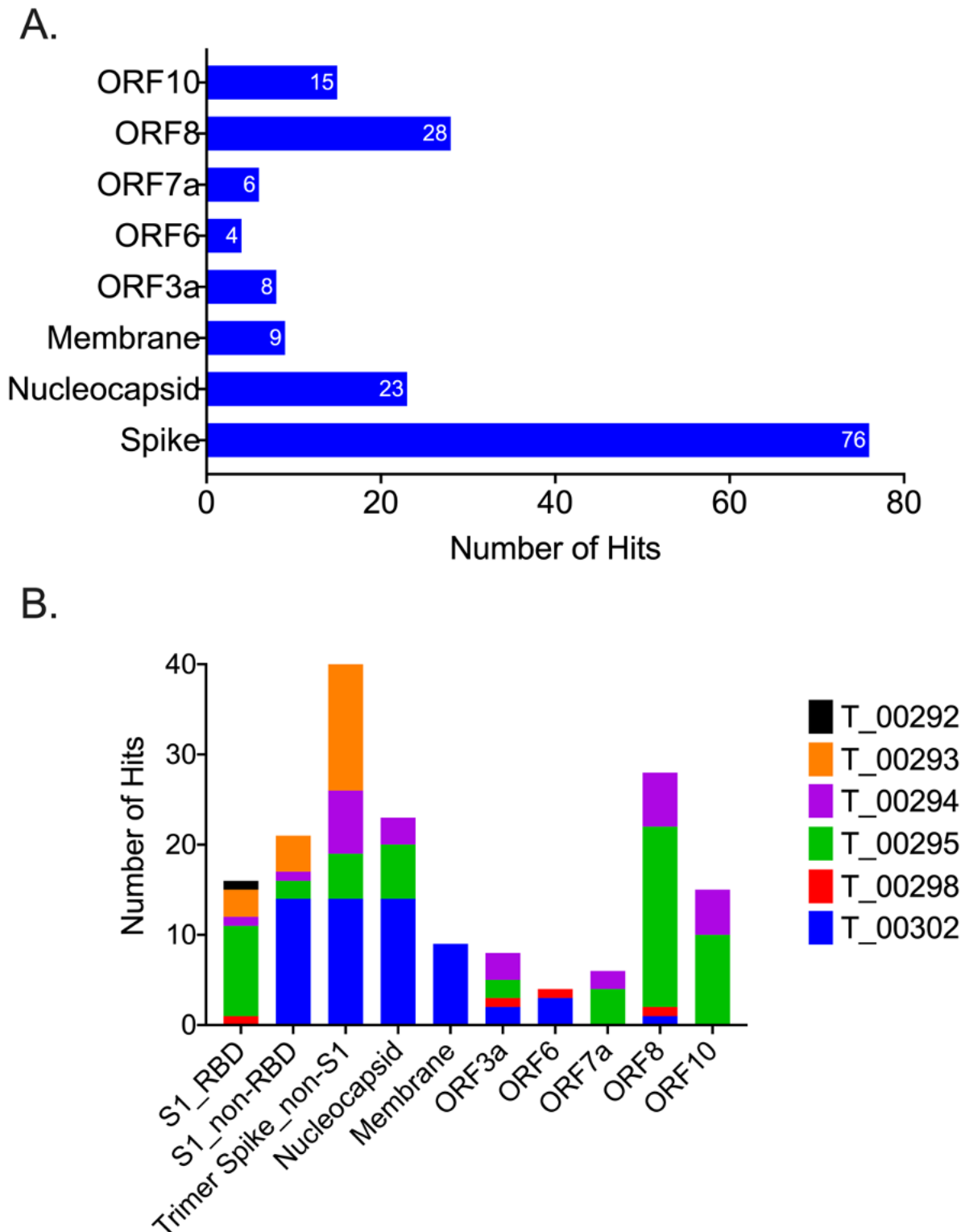178   of antigens being evaluated (Figure 4C).

179

Figure 3. Convalescent patients develop a broad immune response to multiple viral proteins. (A) Less than 50% of the antibodies identified by screening the B cell repertoires

12

183   of convalescent patients were specific for Spike protein. (B) Individual patients made

184   antibodies against a broad array of SARS-CoV-2 proteins.
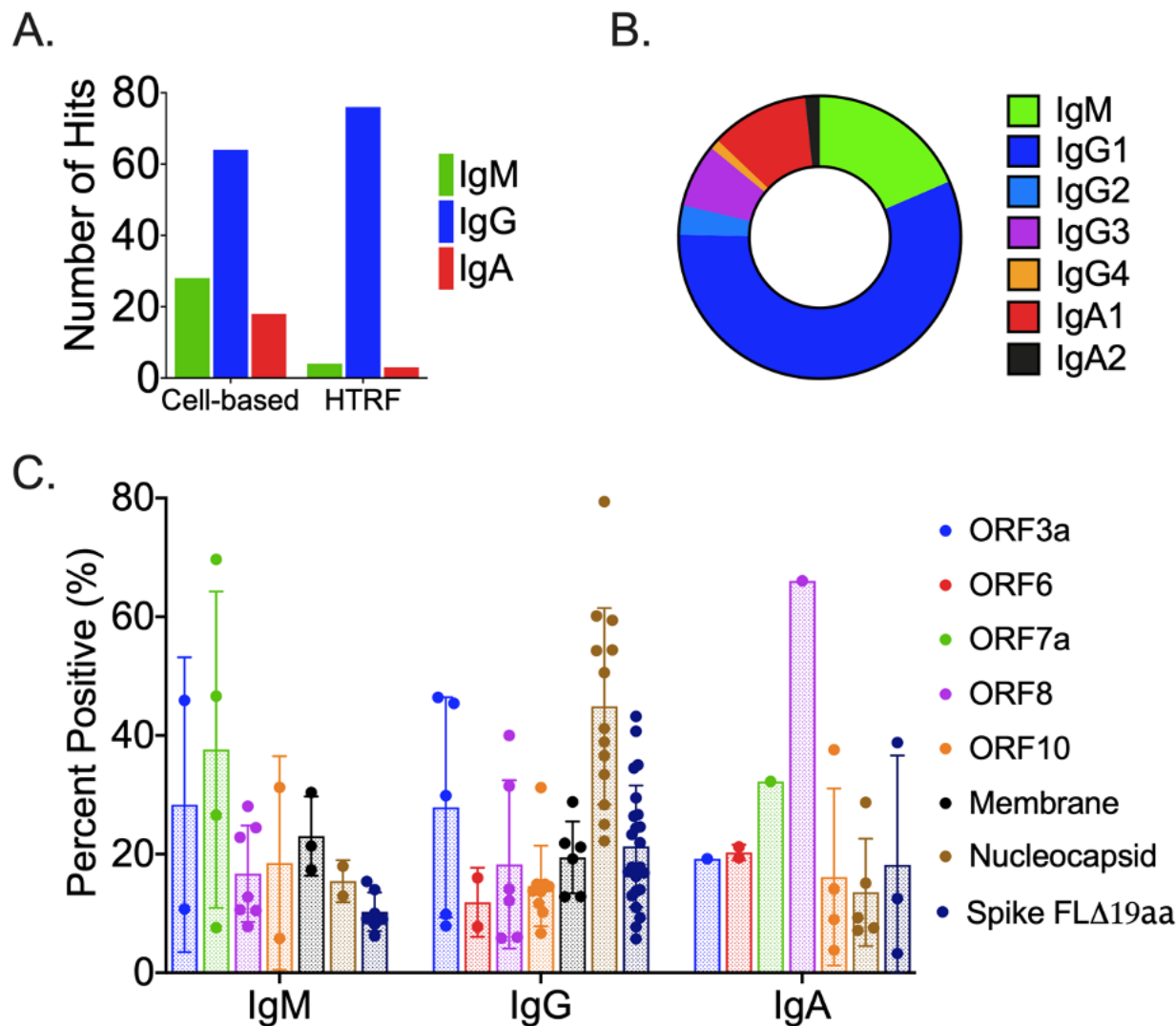
185

186

187   Figure 4. Isotype Distribution of SARS-CoV-2 Specific Antibodies. (A) Distribution

188   identified by the cell- and HTRF-based assays. (B) Distribution of isotypes based upon

189   target. (C) Distribution of isotype sub-classes across targets.

190

191   **Immunoglobulin gene usage in convalescent COVID-19 patients**

13

192

193   We evaluated Ig gene usage in memory B cells of six COVID-19 patients, using an NGS

194   analysis of identified and sequenced 134 hybridoma hits (Figure 5). Two thirds of

195   identified clones used the kappa locus, while the remaining clones used the lambda locus

196   (Figure 5A). Most of the identified VH regions of IgM, IgG and IgA antibodies belonged to

197   IGHV3 gene family (59%), and the rest were from IGHV4 (15.8%), IGHV1 (14.5%), IGHV5

198   (7.2%), IGHV2 (2.9%) and IGHV7 (<1%) gene families (Figure 5B). Although there was

199   no dominant V gene variant, IGHV3-21 (8.6%), IGHV3-33 (7.1%) and IGHV3-48 (6.5%)

200   were among the most abundant identified sequences. The most frequent light chain V

201   regions were IGKV3 (26.6%), IGKV1 (22.3%), IGLV3 (13.67%) and IGLV2 (12.2%)

202   (Figure 5C). Furthermore, sequence analysis of hybridoma hits targeting SARS2 S

203   protein (Figure 5D, E) revealed the significant heterogeneity for V gene usage among B

204   cells that produced anti-viral antibodies. This observation is consistent with the parallel

205   expansion of B cell clones targeting multiple components of the SARS-CoV-2 virus, and

206   points to distinct successful strategies employed by the host adaptive immune response

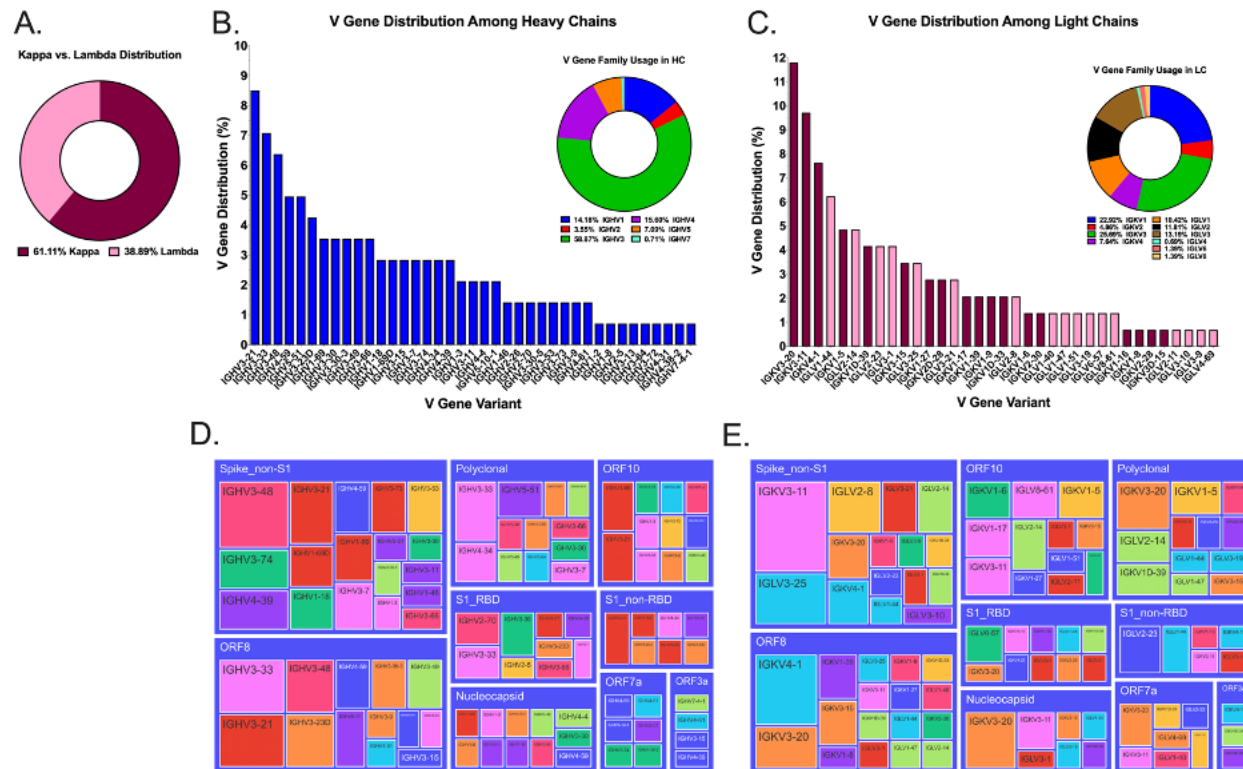207   during its co-evolution with the virus.

208

209

Figure 5. Ig Gene Usage of Identified Screening Hits. (A) Approximately 60% of the identified anti-SARS-CoV-2 screening hits elicited by convalescent patients utilized the kappa light chain locus. (B) VH1 – VH7 gene families were identified as part of antibodies selective for SARS-CoV-2 proteins. (C) Broad range of both kappa and lambda light chains comprise the anti-SARS-CoV-2 primary screening hits isolated by screening the memory B cell repertoires of convalescent patients. (D, E) HC and LC variable domain usage was displayed in a tree diagram using the plotty-express module of the plotty-py program.

Somatic hypermutations in antibodies from high-titer convalescent COVID-19 patients

15

222   We next analyzed heavy and light chain pairs from 103 clones from which we determined

223   productive immunoglobulin RNA sequences. Strikingly, there was a lower-than-expected

224   rate of somatic hypermutation (SHM) in the anti-S antibodies (Figure 6A) and a higher

225   SHM rate in antibodies specific to other viral proteins (ex. N, M, ORF8 and ORF10)

226   (Figure 6A). Of note, even a relatively modest rate of germline mutations in anti-S

227   antibodies resulted in the high affinity Spike-specific antibodies that potently neutralized

228   both S-pseudovirus (Figure 7) and SARS-CoV-2 live virus (manuscript in preparation).

229   Further, a combined analysis of Ig isotype and their level of SHM of virus-specific

230   antibodies revealed several key properties of the productive antiviral response. First,

231   among all "mutated" Igs that had more than 2% of their nucleotide sequence deviated

232   from the closest germline, there was an unusually high (26.4%) proportion of mutated

233   IgMs (Figure 6B), having a mean SHM rate of 5.73%. The functional basis of this

234   phenomenon is not known, but one could speculate that these IgMs came from non-

235   switched memory B cells that had undergone affinity maturation. Second, a subset of

236   such somatically hypermutated IgMs recognized full-length Spike, but not the soluble

237   RBD or S1 subunit of Spike protein. And third, while the predominant isotype among

238   class-switched antibodies was, as expected, IgG (Figure 6C), we were able to capture a

239   panel of fairly mutated virus-specific IgAs. It is plausible that these antibodies play a major

240   role in mucosal neutralization of the incoming virus and may be of particular use for

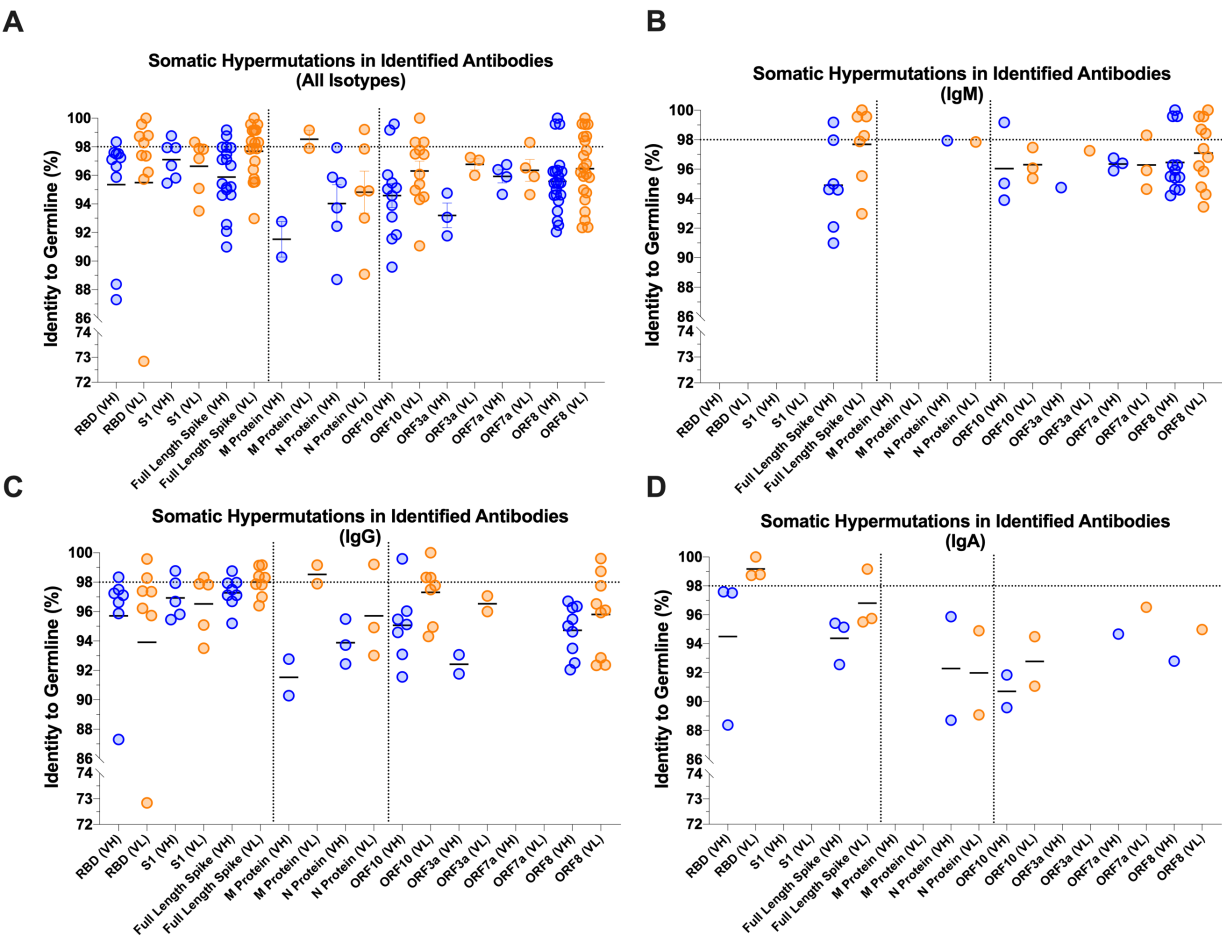241   prophylaxis of viral infection and for vaccine design (Figure 6D).

242

Figure 6. Level of Somatic Hypermutation (SHM) Detected in SARS-CoV-2 Antibodies.
(A) Overall and (B-D) isotype-specific levels of SHM in HC/LC pairs associated with the
primary screening hits specific for individual viral proteins.
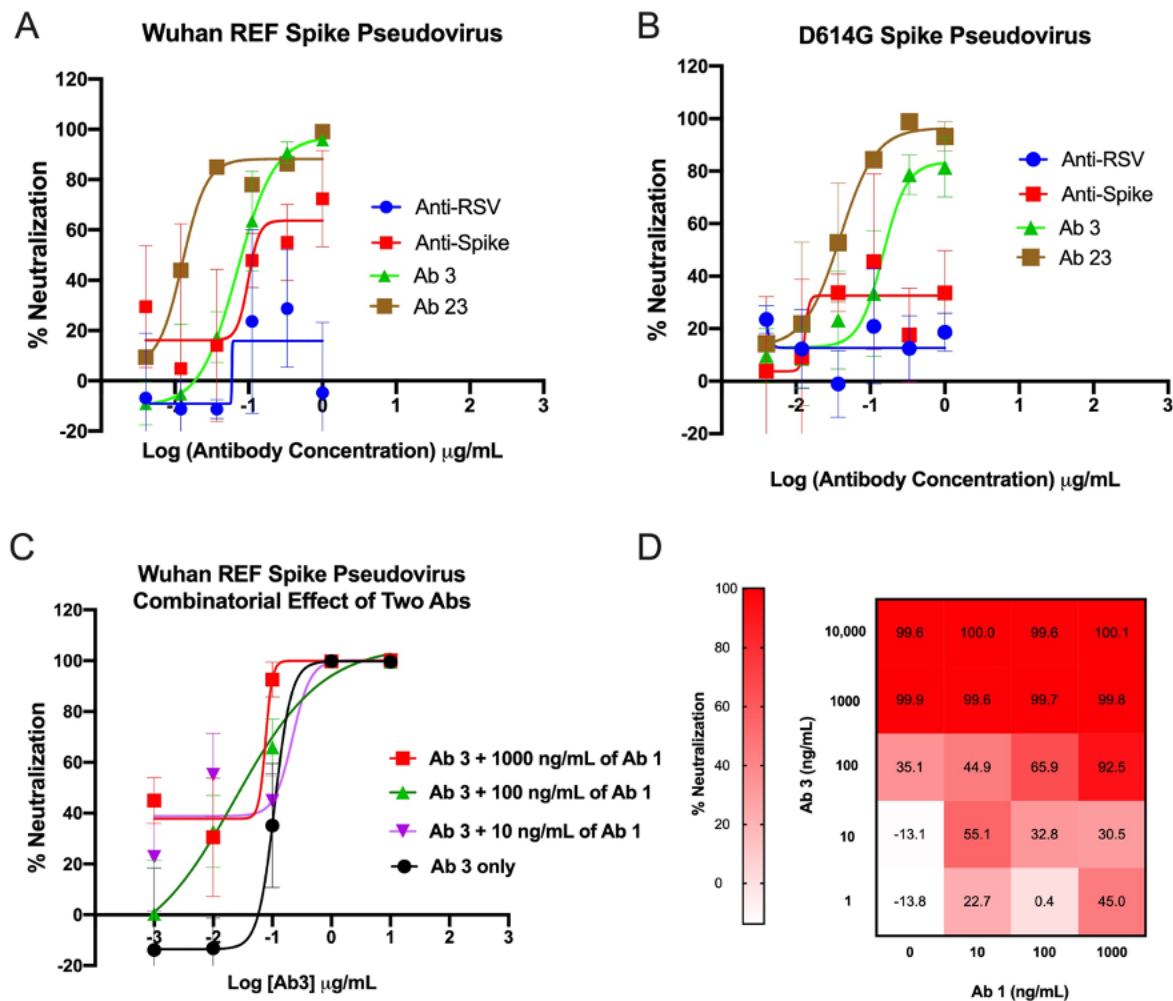
Figure 7. Neutralizing activity of the identified anti-Spike antibodies. (A) Neutralization of WT Spike pseudovirus by selected anti-Spike antibodies. (B) Neutralization of D614G Spike pseudovirus by selected anti-Spike antibodies. (C) Combinatorial effect of Ab#1 and Ab#3 mix on neutralization of WT Spike pseudovirus. (D) Heatmap of percent of neutralization data from panel.

Identified anti-Spike antibodies from convalescent COVID-19 patients exhibit potent neutralizing activity to Spike pseudovirus

18

258 We tested the functional properties of identified anti-Spike antibodies (Figure 7) in a WT

259 and D614G pseudovirus neutralization assay. Spike-expressing pseudoviruses were

260 generated using a lentiviral system and used to infect HEK293 cells overexpressing

261 Angiotensin converting enzyme 2 (ACE2). In the initial screen of antibody-containing

262 supernatants, 3-4 log dilutions of 26 unique anti-Spike antibodies were tested for their

263 ability to block infection in comparison to an anti-RSV negative control and a

264 commercially available anti-Spike positive control. Several antibodies, including Ab#3

265 and Ab#26, potently neutralized pseudovirus infection with EC50 <500 ng/mL (Table 3).

266 Indeed, a full dose response of purified antibodies confirmed strong neutralizing activity

267 of both antibodies (Figure 7A). In addition to the WT (Wuhan) reference strain, various

268 mutations in the Spike protein of SARS-CoV-2 are prevalent throughout the population,

269 with the D614G variant being the dominant strain at the moment of writing of this

270 manuscript [29]. Thus, identified neutralizing antibodies were tested against and

271 neutralized the D614G S pseudovirus with comparable EC_{50} values (Figure 7B). To

272 further enhance neutralizing activity, combinatorial studies looked for any additive

273 effects seen with the addition of anti-Spike antibodies to Ab#3. Ultimately, Ab#1 at

274 various doses was able to enhance neutralizing activity above that of Ab#3 alone

275 (Figure 7C, D).

276

Antibody #	Target (RBD, S1, Trimer S)	in vitro EC$_{50}$ nM (TRF or cell-based assay)		Neutralization potential
		TRF assay	Cell-based assay	
3	RBD, S1, Trimer S	0.015	0.231	HIGH
26	RBD, S1, Trimer S	0.12	0.323	HIGH
10	RBD, S1, Trimer S	0.139	NB	LOW
1	RBD, S1, Trimer S	0.021	1.11	MED
2	RBD, S1, Trimer S	0.025	0.198	MED
15	RBD, S1, Trimer S	0.097	1.04	MED
4	S1, Trimer S	0.015	0.434	LOW
5	S1, Trimer S	0.111	0.198	LOW
13	S1, Trimer S	0.054	0.421	MED
6	Trimer S	NB	1.18	MED
Anti-Spike (+)	RBD, S1, Trimer S	0.904	ND	0.316 µg/mL
Anti-RSV (-)	N/A	NB		14.125 µg/mL
		LOW: neutralization is comparable or below to anti-RSV		
		MED: neutralization is observed, but inferior to anti-Spike (Sino Bio)		
		HIGH: neutralization is superior to anti-Spike (Sino Bio)		
		NB: not binding detected		
		ND: not determined		

Table 3: Binding properties of anti-Spike antibodies

DISCUSSION

The SARS-CoV-2 pandemic has stimulated extraordinary efforts to study anti-viral response and to develop means for treatment and prophylaxis, in both the academic and the biopharmaceutical research communities. By the end of October 2020, a mere 11 months after the virus was first identified, the Clinicaltrials.gov database listed more than 3500 distinct clinical trial activities directed at patients infected with SARS-CoV-2. There is significant diversity among these efforts, from the assessment of existing drugs, to the use of convalescent plasma from recovered patients, to the use of specific vaccines and antibodies directed at the viral S protein. It is not yet apparent that there will be a single

20

290 approach that will prove to be uniformly effective at preventing viral infections or

291 accelerating viral clearance in all groups of COVID-19 patients.

292

293 It is possible that even the most effective approaches will have limited or unsustainable

294 efficacy. The vast majority of the ongoing efforts are all targeting the S protein. Both

295 passive (therapeutic antibodies) and active (vaccine) approaches directed at S protein

296 are expected to promote virus neutralization, that is, inhibition of viral entry into healthy

297 cells. Unfortunately, a mutation in S protein has already been reported [20,21] and further

298 mutations may ultimately limit the effectiveness of therapies directed at this single protein

299 [22].

300 Given the multiplicity of SARS-CoV-2 proteins that induce antigen-specific T and B cell

301 responses in humans, it is reasonable that an unbiased interrogation of the memory B

302 cells generated by high-titer, convalescent COVID-19 patients could identify high-affinity

303 Igs directed at specific viral antigens. As an outcome of this approach, there was not a

304 single dominant V gene LC/HC combination specific to a particular viral protein among

305 characterized 134 Igs from convalescent patients. In fact, sequence analysis revealed a

306 lower rate of SHM of anti-Spike Igs than of antibodies directed at other viral proteins (N,

307 M, ORF8 and ORF10). Remarkably, even a modest rate of germline mutations in anti-S

308 antibodies resulted in potent neutralization of both S-expressing pseudovirus (Figure 7)

309 and SARS-CoV-2 live virus (manuscript in preparation). To our surprise, these Spike-

310 specific antibodies included an atypically high proportion of well-mutated anti-viral IgMs

311 (26.4% with a mean mutation rate of 5.73%) suggesting that non-switched memory B

312 cells also undergo affinity maturation in response to SARS-CoV-2 infection. Further, a

313   subset of such mutated IgMs targeted the full-length Spike, but not soluble S1 or RBD

314   domains. The identification of IgG and IgA antibodies specific for the full range of targets

315   screened, including the RBD domain of S, highlights the requirement of additional events,

316   such as immunoglobulin class switching, for the development of a productive neutralizing

317   antibody response. Finally, and perhaps not unexpectedly, we have identified a group of

318   polyreactive antibodies (data not shown). A relatively high rate of SHM in these

319   polyreactive antibodies may suggest a secondary maturation event that redirected

320   immature B cell clones toward SARS-CoV-2 antigens.

321

322   The majority of anti-S antibodies, as expected, recognized a full-length S protein (Table

323   3). Further, all but one of the six COVID-19 convalescent patients produced antibodies to

324   a soluble receptor-binding domain of S protein (RBD). Of note, while most of the RBD-

325   and S1-specific antibodies were less mutated than those specific to the full-length S

326   protein, we identified several highly mutated RBD-specific outliers. Lower rate of SHM in

327   the S-specific antibody group may connote limited rounds of affinity-maturation for a high

328   antigenic protein. These anti-Spike antibodies demonstrated functional activity in a

329   pseudovirus neutralization assay. In fact, there were several potent neutralizing

330   antibodies (e.g., Ab#3, Ab#26), that had EC_{50} in 100 ng/mL range. One of these two

331   antibodies demonstrated a combinatorial effect with Ab#1 in pseudovirus (Figure 7C, D)

332   neutralization assays. The selectivity, affinity, and functional activity of the anti-Spike

333   antibodies suggest that they were a part of the successful anti-viral responses mounted

334   by the patients from which they were derived. By extension, the antibodies identified

335   against other viral targets may have also contributed to the viral clearance through

336   mechanisms other than neutralization (i.e., activators of complement and/or effector

337   cells).

338

339   In summary, an unbiased interrogation of the B cell repertoires of convalescent COVID-

340   19 patients demonstrated that these patients make a strong humoral response against a

341   broad array of SARS-CoV-2 proteins. These responses included high affinity antibodies

342   of multiple Ig isotypes. The natural immune response to SARS-CoV-2 among these

343   patients stands in stark contrast to the anti-S focused approaches being taken to develop

344   therapeutic antibodies to treat COVID-19. An alternative approach should include

345   targeting a breadth of SARS-CoV-2 proteins with a cocktail of antibodies, with the

346   anticipation that a multi-targeted mixture will be more effective at inducing robust viral

347   clearance via neutralization and Fc-mediated activation of complement and effector cells.

348

349   **MATERIAL AND METHODS**

350

351   **Cells**

352

353   293TN Producer cell line (System Biosciences, Cat #LV900A-1) was maintained in

354   DMEM containing 10% FBS. HEK293 cells expressing human Angiotensin converting

355   enzyme 2 (ACE2) (BPS Biosciences, Cat #79951) were cultured in EMEM containing

356   10% FBS and 5 mg/mL Puromycin to select for ACE2-expressing cells. ACE2

357   expression was confirmed by flow cytometry. Cells were detached with CellStripper

358   (Corning, Cat # 25-056-Cl) and labeled with LIVE/DEAD Aqua (Invitrogen, Cat #

359   L34966) at 1:1000 dilution at room temperature for 10 minutes. After that, cells were

360   washed twice in PBS and stained with a goat anti-human ACE2 polyclonal antibody

361   (R&D Systems, Cat # AF933) or isotype goat polyclonal isotype control (R&D Systems,

362   Cat # AB-108-C) at 1:100 dilution for 30 minutes on ice. Next, cells were washed twice

363   and stained with Alexa Fluor 488-conjugated donkey anti-goat antibody (Jackson

364   ImmunoResearch, Cat #705-545-147) at 1:200 dilution for 30 minutes on ice. Finally,

365   cells were washed twice and run on the Attune NxT (ThermoFisher). Data were

366   analyzed using FlowJo software (BD).

367

368

369   **Collection of patient samples**

370

371   Blood samples were drawn from six convalescing COVID-19 patient volunteers deemed

372   eligible   for   donating   convalescent   plasma   as   set   forth   in   the   US   FDA's

373   Recommendations [23]. Patients displayed no PCR-detectable viremia and maximal IgG

374   (2880) titer of class-switched, virus-specific antibodies. Donors gave written consent to

375   have their blood drawn and authorized the unrestricted use of their blood samples by

376   Immunome.   The samples were deidentified and the B cells were isolated from those

377   deidentified blood samples. Immunome did not seek IRB approval of a "research project"

378   because   analysis   of   peripheral   blood   samples   that   are   obtained   with   consent,

379   deidentified,   coded   or   anonymized   are   not   believed   to   be   subject   to   human   tissue

380   research regulations. Immunome used a commercial vendor to obtain additional blood

381   samples, one with a standing IRB approval in place for their donor collection efforts.

382

383

Generation of hybridoma libraries

Hybridomas were generated following protocols for isolating and expanding primary B-cells as well as electrofusion methods described in U.S. patents [24,25]. Hybridomas stably expressing human mAbs were generated by electrofusion of expanded B-cells to the B5-6T myeloma cell line, which expresses an ectopic human telomerase gene that stabilizes human chromosomes in the hybrid cells created. Fused hybridomas were plated into 96-well plates in growth medium with HAT selection of stable hybridomas for 7 days. After 7 days, growth media were switched to media with HT for stable selected hybridoma growth. Hybridomas were cultured in a 37°C incubator for 14-21 days during which time they were imaged for monoclonality and monitored for isotype-and sub-class-specific Ig secretion. Supernatants from monoclonal wells expressing measurable levels of Ig were cherry-picked and submitted for target-based screening.

HTRF Screening Assays

A homogeneous time-resolved fluorescence (hTRF) assay [26] comprised of terbium-labeled anti-human IgG (H+L) (Cisbio, custom label) donor and AF488-labeled anti-HIS (Cell Signaling, Cat # 14930S) acceptor antibodies was used to screen patient-derived antibodies for their binding to recombinantly produced SARS-CoV-2 antigens. The assay, adapted for high-throughput screening, was optimized so that a number of recombinant, HIS-tagged SARS-CoV-2 target proteins could be substituted interchangeably. This

404 recombinant target panel consisted of two full-length viral structural proteins, S (FL,

405 trimer-stabilized, LakePharma) and N (GenScript); two truncated S protein domains, S1

406 (GenScript, Cat # Z03485-1) and RBD (aa 319-591, LakePharma); and two ORF proteins,

407 ORF3a (ProSci, Cat # 10-005) and ORF8 (ProSci, Cat # 10-002). Commercially available

408 antibodies specific for the individual structural viral proteins, SARS-CoV/SARS-CoV-2

409 Spike S1 (RBD) chimeric mAb (Sino Biological, Cat # 40150-D001), SARS CoV-2

410 Nucleocapsid human chimeric mAb (GenScript, Cat # A02039-100), or in-house

411 antibodies to ORF3a and ORF8 served as positive controls. Assay background was

412 determined by averaging the signal of wells containing only the donor and acceptor

413 cocktail. Hybridoma supernatants exhibiting signals greater than 2-fold over background

414 were reported as positive HITs and are submitted for Ig sequence analysis.

415

416 <u>Flow cytometry-based cellular screens for antiviral antibodies</u>

417

418 SARS-CoV-2 antigen sequences were cloned into pcDNA3.4 plasmids and transfected

419 into 293F cells utilizing the Expi293 Expression System (Life Technologies, Cat #

420 A14635) per manufacturer's instructions. Cells expressing SARS-CoV-2 N, ORF6, ORF8,

421 and ORF10 proteins were transferred into Expi293 Expression medium (Life

422 Technologies, Cat # A1435103) under antibiotic (Geneticin) selection (Gibco, Cat #

423 10131027) for 3-5 days following transfection to establish individual stable cell pools. The

424 stable cells were maintained under selection in the presence of Geneticin. Protein

425 localization was confirmed by flow cytometry for either intact or fixed and permeabilized

426 Intracellular Perm Buffer (BioLegend, Cat # 421002)) cells. Cells transiently expressing

427   SARS-CoV-2 S (S delta 19aa), M, ORF3a, and ORF7a were included in the screening

428   panel. Optimal protein expression was achieved two days post-transfection for ORF3a

429   and ORF7a and three days post-transfection for S and M proteins.

430

431   For both the cell-surface binding and intracellular detection assays, cells were incubated

432   with LIVE/DEAD Cell Stain kit (ThermoFisher, Cat # L34960) per the manufacturer's

433   instructions. For cell surface binding, live cells expressing S delta 19aa were suspended

434   in QSol Buffer (IntelliCyte Corporation) to which a cocktail of Fc-specific secondary

435   antibodies was added: AF647 goat anti-human IgG (Jackson ImmunoResearch, Cat #

436   109-605-008), AF488 goat anti-human IgA (Jackson ImmunoResearch, Cat # 109-115-

437   011) and BV650 mouse anti-human IgM (BioLegend, Cat # 314526).

438

439   For the permeabilization assay, stained cells were first fixed with paraformaldehyde

440   (BioLegend, Cat # 420801) at a final concentration of 1%. Fixed cells were then

441   permeabilized with Intracellular Permeabilization Buffer (BioLegend) according to the

442   manufacturer's instructions. A cocktail of Fc-specific secondary antibodies consisting of

443   AF647 goat-anti-human IgG (Jackson ImmunoResearch, Inc.), PE goat-anti-human IgA

444   (Jackson ImmunoResearch, Inc.), and BV650 mouse-anti-human IgM (BioLegend) was

445   added to cell suspension.

446

447   For each assay, the cell suspensions were dispensed into 384-well plates, followed by

448   the addition of hybridoma supernatant at a 1:10 final dilution. The reaction was allowed

449   to incubate for 90 minutes at room temperature. For the permeabilization assay, plates

450   were centrifuged, and cell pellets were suspended in QSol Buffer (IntelliCyte

451   Corporation). Cells for each assay were fixed with a final concentration of 1%

452   paraformaldehyde and analyzed with IntelliCyte iQue Screener (IntelliCyte Corporation).

453   Positive binding gates for detection of each secondary antibody were established using

454   cells plus secondary antibody cocktail as a negative control. Binding of hybridoma

455   supernatant antibodies to specific SARS-CoV-2 proteins was quantified as percent

456   positive relative to the secondary only control. To calculate percent positive, live events

457   that shifted into detection channels were divided by the total live events.

458

459   <u>RNA isolation and Next Generation Sequencing (NGS)</u>

460   Hybridoma RNA was isolated using RNAqueous-96 Total RNA Isolation Kit (Invitrogen,

461   Cat # AM1920). Isolated RNA samples were submitted to iRepertoire (Huntsville, AL) for

462   NGS. Hybridoma-derived RNA samples were sequenced using the Illumina MiSeq

463   system at iRepertoire (Huntsville, AL). Sequencing runs were performed using the MiSeq

464   Nano Kit V2 following bead-based cleanup of RNA. Immunoglobulin sequences

465   containing CDR1, 2 and 3 and framework regions were amplified using IgG and IgA-

466   specific mixes for IgH, and kappa and lambda-specific primers for IgL. IgM-expressing

467   hybridoma samples, from which IgG or IgA heavy chains were not amplified using this

468   approach, were sequenced using the iRepertoire iPair system. Final sequences were

469   exported using iPair software.

470   The analysis of primary NGS data was performed by iRepertoire. Immunoglobulin

471   sequences were analyzed for predicted CDR sequences, % identity to appropriate

472   germlines, isotype of the constant regions and read counts. Sequence pairing was

28

473   performed based on the read count information. In the event more than one LC:HC pair

474   was discovered in a single well, each LC:HC combination was analyzed as a separate

475   antibody. In wells exhibiting 5' truncation in the V region, the germline sequence was used

476   to create an expression construct. Final sequences were translated and analyzed for

477   potential stop codons and frame shifts.

478   Production of paired light and heavy chains

479   Variable domains yielding productive uninterrupted protein sequences were analyzed for

480   number of reads and the degree of somatic hypermutations (SHM) in comparison to the

481   closest immunoglobulin germline. Hybridoma hit sequences with at least one chain that

482   had more than 2% of SHM were advanced to HC/LC pairing and the recombinant

483   production of antibodies. Immunoglobulin expression fragments were cloned into the

484   pcDNA3.4-based vectors and expressed in 293F cells. Affinity and binding pattern of

485   recombinant antibodies were compared to the original antibody-containing hybridoma

486   supernatants in BLI, HTRF and cell-based assay. Antibody-containing supernatants or

487   purified antibodies were advanced to downstream assays. If multiple heavy or light chain

488   sequences were detected within one well, their CDRs were aligned and compared for

489   potential PCR errors. In cases where multiple sequences within a well were different, i.e.,

490   originated from separate clones, all potential combinations of light and heavy chains were

491   recombinantly produced and tested in downstream assays. Wells that yielded a single

492   HC/LC pair were advanced to recombinant expression and downstream assays. 5'

493   fragments of the constant regions were sequenced to identify the isotype of the antibody

494   and compared to the experimentally identified isotype of hybridoma supernatants. The

495   resulting isotype of the heavy or light chain was assigned based on two or more positive

496   readings from experimental (ex. ELISA and FACS) assays and sequencing.

497

498   **Pseudovirus Production and Neutralization Assay**

499

500   Spike-expressing pseudovirus was generated with System Bioscience's pPACK-SPIKE

501   packaging system (System Biosciences, Cat # CVD19-50A-1) as per manufacturer's

502   protocol. Briefly, $8x10^6$ 293TN Producer cells (System Biosciences, Cat # LV900A-1)

503   were plated in T150 flasks overnight. Plasmids encoding lentiviral packaging proteins

504   and Spike were added 1mL of plain DMEM for each T150 being transfected. 55 mL of

505   PureFection reagent (System Biosciences; Cat # LV750A-1) was added to each 1mL

506   tube, vortexed for 10 seconds, and incubated at room temperature for 15 minutes. The

507   plasmid and PureFection mixture was added to a T150 flask containing 293TN cells and

508   placed in a 37°C incubator containing 5% CO_2 for 48 hours. Pseudovirus-containing

509   supernatants were harvested at 48 hours and passed through a 0.45-micron PVDF filter

510   to remove cellular debris. 5x PEG-it Virus Precipitation Solution (System Biosciences,

511   Cat # LV810A-1) was added to supernatants and incubated 4°C overnight.

512   Pseudovirus-containing supernatants containing 1x PEG-it Virus Precipitation Solution

513   were then spun at 1500 x g for 30 minutes. Pseudovirus-containing pellets were

514   resuspended in plain DMEM to achieve at 10x concentration and frozen at -80°C in

515   single use aliquots.

516

517   Pseudovirus infection and neutralization assays were performed by adapting

518   established protocols [27, 28]. In summary, 10^4 ACE2-293T cells were plated in the

519   inner 60 wells of a 96 well flat bottom plate in 100uL of ACE2-293T media overnight in a

520   37°C incubator containing 5% CO_2. To determine infectivity of each lot of pseudovirus,

521   pseudovirus-containing supernatants were thawed from -80°C and two-fold dilutions

522   were performed. 100 mL of pseudovirus at various dilutions was added to ACE2-293T

523   cells. To test neutralization activity of antibodies, indicated antibody concentrations

524   were pre-incubated with pseudovirus for 1 hour in a 37°C incubator containing 5% CO_2.

525   Then, 100 mL of antibody/pseudovirus mixture was added to ACE2-293T cells. After 72

526   hours, cells and media were equilibrated to room temperature for 20 minutes. 100 mL

527   of media was removed and replaced with 100 mL of Bright-Glo Luciferase Assay

528   Reagent (Promega, Cat # E2620). Luciferase activity was measured on the EnSpire

529   Plate Reader (PerkinElmer). Percent neutralization was calculated using RLUs with the

530   equation [(RLU of Virus + cells) – (RLU of Experimental Sample)] / [(RLU of Virus +

531   cells) – (RLU of cells only)].

532

533

534   **ACKNOWLEDGEMENTS**

535

540   under contract W911QY2090019. The opinions, interpretations, conclusions and

541   recommendations are those of the authors and are not necessarily endorsed by the U.S.

542   Army.

543

544

REFERENCES

1. Zhou P, Yang X Lou, Wang XG, Hu B, Zhang L, Zhang W, et al. A pneumonia outbreak associated with a new coronavirus of probable bat origin. Nature. 2020;579: 270–273. doi:10.1038/s41586-020-2012-7

2. Editorial. Progress report on the coronavirus pandemic. Nature. 2020;584: 325–325. Available: https://media.nature.com/original/magazine-assets/d41586-020-02414-1/d41586-020-02414-1.pdf

3. Morens DM, Fauci AS. Emerging Pandemic Diseases: How We Got to COVID-19. Cell. Cell Press; 2020. pp. 1077–1092. doi:10.1016/j.cell.2020.08.021

4. Chakraborty I, Maity P. COVID-19 outbreak: Migration, effects on society, global environment and prevention. Sci Total Environ. 2020;728: 138882. doi:10.1016/j.scitotenv.2020.138882

5. WHO Coronavirus Disease (COVID-19) Dashboard | WHO Coronavirus Disease (COVID-19) Dashboard. [cited 9 Nov 2020]. Available: https://covid19.who.int/?gclid=Cj0KCQiA7qP9BRCLARIsABDaZzhj4p4n5emnuHTO24B5Wi-N10YYvhUbGPsXFht_Cmcim1HjG7fLuV0aAn_iEALw_wcB

6. Berlin DA, Gulick RM, Martinez FJ. Severe Covid-19. N Engl J Med. 2020 [cited 5 Nov 2020]. doi:10.1056/nejmcp2009575

7. Fehr AR, Perlman S. Coronaviruses: An overview of their replication and

565   pathogenesis. Coronaviruses: Methods and Protocols. Springer New York; 2015.

566   pp. 1–23. doi:10.1007/978-1-4939-2438-7_1

567   8.   Lan J, Ge J, Yu J, Shan S, Zhou H, Fan S, et al. Structure of the SARS-CoV-2

568   spike receptor-binding domain bound to the ACE2 receptor. Nature. 2020;581:

569   215–220. doi:10.1038/s41586-020-2180-5

570   9.   Robbiani DF, Gaebler C, Muecksch F, Lorenzi JCC, Wang Z, Cho A, et al.

571   Convergent Antibody Responses to SARS-CoV-2 Infection in Convalescent

572   Individuals. bioRxiv. 2020; 2020.05.13.092619. doi:10.1101/2020.05.13.092619

573   10.   Braun J, Loyal L, Frentsch M, Wendisch D, Georg P, Kurth F, et al. SARS-CoV-2-

574   reactive T cells in healthy donors and patients with COVID-19. Nature. 2020.

575   doi:10.1038/s41586-020-2598-9

576   11.   Ferretti AP, Kula T, Wang Y, Nguyen DMV, Weinheimer A, Dunlap GS, et al.

577   Unbiased Screens Show CD8+ T Cells of COVID-19 Patients Recognize Shared

578   Epitopes in SARS-CoV-2 that Largely Reside outside the Spike Protein. Immunity.

579   2020 [cited 5 Nov 2020]. doi:10.1016/j.immuni.2020.10.006

580   12.   Cao Y, Su B, Guo X, Sun W, Deng Y, Bao L, et al. Potent neutralizing antibodies

581   against SARS-CoV-2 identified by high-throughput single-cell sequencing of

582   convalescent patients' B cells. Cell. 2020. doi:10.1016/j.cell.2020.05.025

583   13.   Grifoni A, Weiskopf D, Ramirez SI, Mateus J, Dan JM, Moderbacher CR, et al.

584   Targets of T Cell Responses to SARS-CoV-2 Coronavirus in Humans with

585   COVID-19 Disease and Unexposed Individuals. Cell. 2020;181: 1489-1501.e15.

586   doi:10.1016/j.cell.2020.05.015

587   14.   Stamper CT, Dugan HL, Li L, Asby NW, Halfmann PJ, Guthmiller JJ, et al. Distinct

588   B cell subsets give rise to antigen-specific antibody responses against SARS-

589   CoV-2. Res SquareResearch Sq. 2020. Available:

590   https://europepmc.org/articles/PMC7523131

591   15.   Puligedda RD, Kouiavskaia D, Adekar SP, Sharma R, Devi Kattala C, Rezapkin

592   G, et al. Human monoclonal antibodies that neutralize vaccine and wild-type

593   poliovirus strains. Antiviral Res. 2014;108: 36–43.

594   doi:10.1016/j.antiviral.2014.05.005

595   16.   Puligedda RD, Kouiavskaia D, Al-Saleem FH, Kattala CD, Nabi U, Yaqoob H, et

596   al. Characterization of human monoclonal antibodies that neutralize multiple

597   poliovirus serotypes. Vaccine. 2017;35: 5455–5462.

598   doi:https://doi.org/10.1016/j.vaccine.2017.03.038

599   17.   Puligedda RD, Vigdorovich V, Kouiavskaia D, Kattala CD, Zhao J, Al-Saleem FH,

600   et al. Human IgA Monoclonal Antibodies That Neutralize Poliovirus, Produced by

601   Hybridomas and Recombinant Expression. Antibodies. 2020;9: 5.

602   doi:10.3390/antib9010005

603   18.   Tursi SA, Puligedda RD, Szabo P, Nicastro LK, Miller AL, Qiu C, et al. Salmonella

604   Typhimurium biofilm disruption by a human antibody that binds a pan-amyloid

605   epitope on curli. Nat Commun. 2020;11: 1007. doi:10.1038/s41467-020-14685-3

606   19.   Levites Y, O'Nuallain B, Puligedda RD, Ondrejcak T, Adekar SP, Chen C, et al. A

607   human monoclonal IgG that binds Aβ assemblies and diverse amyloids exhibits

608   anti-amyloid activities in vitro and in vivo. J Neurosci. 2015;35: 6265–6276.

609   doi:10.1523/JNEUROSCI.5109-14.2015

610 20. Li Q, Wu J, Nie J, Zhang L, Hao H, Liu S, et al. The Impact of Mutations in SARS-

611   CoV-2 Spike on Viral Infectivity and Antigenicity. Cell. 2020;182: 1284-1294.e9.

612   doi:10.1016/j.cell.2020.07.012

613 21. Korber B, Fischer WM, Gnanakaran S, Yoon H, Theiler J, Abfalterer W, et al.

614   Tracking Changes in SARS-CoV-2 Spike: Evidence that D614G Increases

615   Infectivity of the COVID-19 Virus. Cell. 2020;182: 812-827.e19.

616   doi:10.1016/j.cell.2020.06.043

617 22. Callaway BE. The coronavirus is mutating — does it matter? Nature. 2020;585.

618   Available: https://www.nature.com/articles/d41586-020-02544-6

619 23. FDA. Guidance for Industry: FDA's Recommendations for Investigational COVID-

620   19 Conavalescent Plasma. FDA; 2020. Available:

621   https://www.fda.gov/media/136798/download

622 24. Dessain SK., Weinberg RA. US7491530B2. 2002. Available:

623   https://patentimages.storage.googleapis.com/ad/55/26/a3d7080031c38a/US7491

624   530.pdf

625 25. Dessain SK, Adekar SP. US8999707B2. 2009. Available:

626   https://patentimages.storage.googleapis.com/ad/55/26/a3d7080031c38a/US7491

627   530.pdf

628   26.   Degorce F, Card A, Soh S, Trinquet E, Knapik GP, Xie B. HTRF: A technology

629   tailored for drug discovery - A review of theoretical aspects and recent

630   applications. Current Chemical Genomics. 2009. pp. 22–32.

631   doi:10.2174/1875397300903010022

632   27.   Crawford KHD, Eguia R, Dingens AS, Loes AN, Malone KD, Wolf CR, et al.

633   Protocol and Reagents for Pseudotyping Lentiviral Particles with SARS-CoV-2

634   Spike Protein for Neutralization Assays. Viruses. 2020;12: 513.

635   doi:10.3390/v12050513

636   28.   Du, L., Zhang, X., Liu, J. & Jiang, S. Protocol for recombinant RBD-based SARS

637   vaccines: protein preparation, animal vaccination and neutralization detection. J

638   Vis Exp Jove (2011) doi:10.3791/2444

639   29.   Plante, J. A. et al. Spike mutation D614G alters SARS-CoV-2 fitness. Nature 1–9

640   (2020) doi:10.1038/s41586-020-2895-3.

641

642

643